

RESEARCH

Open Access



# Constitutive Model for Aggregate Interlock in FEM Analyses of Concrete Interfaces with Embedded Steel Bars

Diogo Figueira<sup>1</sup>, Carlos Sousa<sup>2\*</sup> and Afonso Serra Neves<sup>2</sup>

## Abstract

A nonlinear finite element model (FEM) is developed to assess the behaviour of a cracked concrete interface, reinforced with embedded steel bars and subjected to monotonic loading. A dowel action finite element modelling approach is conceived for that purpose. The bond between the steel bars and the surrounding concrete is also considered in the model and an interface finite element is included to simulate aggregate interlock. Then, the comparison of the model results with experimental values allowed the calibration of aggregate interlock constitutive relations for cracks in monolithic concrete restrained by embedded steel bars. New constitutive relations are also proposed for shear transfer by aggregate interlock in a concrete joint.

**Keywords:** aggregate interlock, finite element analysis, reinforced concrete, shear

## 1 Introduction

Concrete to concrete interfaces arise when a discrete crack occurs in monolithic concrete or when two concretes cast at different times are in contact forming a concrete joint (Dias-da-Costa et al. 2012; Fang et al. 2018; Kim et al. 2018; Rndl 2013). In the case of a concrete joint, adhesion between the concretes is the main strength mechanism before cracking (Espeche and León 2011; Mohamad et al. 2015; Saldanha et al. 2013; Xu et al. 2015). After cracking, the shear stress transfer through a reinforced concrete interface (Haskett et al. 2011; Santos and Júlio 2014) can be modelled as the superposition of two different strength mechanisms: dowel action of the reinforcing bars (Millard and Johnson 1984; Rndl 2007; Vintzileou and Tassios 1986) and aggregate interlock (Niwa et al. 2016; Rahal et al. 2016).

The numerical finite element (FE) modelling of the dowel action mechanism in a concrete interface was

recently discussed in Figueira et al. (2018). The simulation of the steel/concrete interface nonlinear behaviour throughout the reinforcing bar length is the main improvement of the modelling approach proposed in Figueira et al. (2018) when compared to other finite element dowel action models currently available in literature (Kwan and Ng 2013; Magliulo et al. 2014; Moradi et al. 2012; Zoubek et al. 2014).

In terms of the aggregate interlock mechanism, FE modelling was implemented by Feenstra et al. (1991a, b) for a single interface element and for assemblies of interface elements and plane-stress elements. Five proposals for aggregate interlock modelling were considered by Feenstra et al. (1991a, b). Three empirical: 'rough crack model' by Bazant and Gambarova (1980), 'rough crack model' by Gambarova and Karakoç (1983) and the aggregate interlock constitutive relations of Walraven and Reinhardt (1981); and two physical: 'contact density model' by Li et al. (1989) and the 'two phase model' by Walraven (1981).

By comparing them with the experimental data of Paulay and Loeber (1974) and Walraven et al. (1979), Feenstra et al. (1991a, b) verified that the aggregate interlock relations (Walraven and Reinhardt 1981)

\*Correspondence: cfsousa@fe.up.p

<sup>2</sup> CONSTRUCT-LABEST, Faculty of Engineering (FEUP), University of Porto,

Rua Dr. Roberto Frias, s/n, 4200-465 Porto, Portugal

Full list of author information is available at the end of the article

Journal information: ISSN 1976-0485 / eISSN 2234-1315

had the best behaviour. Such relations allowed the use of a tangential stiffness matrix in the iteration method even for very low displacement values. Moreover, in those aggregate interlock relations, a full Newton–Raphson procedure always resulted in converged solutions and large load steps were possible even for small displacements in the interface. The relations are the following:

$$\tau_{\text{agg}} = C_f \left\{ -0.0333 f_{cc} + \left[ 1.8w^{-0.8} + (0.234w^{-0.707} - 0.20)f_{cc} \right] s \right\} \quad (1)$$

$$\sigma_n = C_f \left\{ -0.05 f_{cc} + \left[ 1.35w^{-0.63} + (0.191w^{-0.552} - 0.15)f_{cc} \right] s \right\} \quad (2)$$

where  $\tau_{\text{agg}}$  is the shear stress due to aggregate interlock and  $\sigma_n$  the normal stress on the interface. Slip  $s$  and crack opening  $w$  should be in mm, while stresses  $f_{cc}$  (concrete compressive strength measured in cubic specimens),  $\sigma_n$  and  $\tau_{\text{agg}}$  should be in MPa. In turn,  $C_f$  is an aggregate effectiveness coefficient that should be taken as 0.35 if the crack crosses the aggregates and 1.0 otherwise.

The empirical relations of Eqs. (1) and (2) were obtained from tests on cracks in monolithic concrete restrained by external steel bars. To the authors' knowledge, no proposal exists in the literature to adapt this type of aggregate interlock relations for other interface roughness profiles or for interfaces with embedded bars. In this regard, aggregate interlock relations for interfaces with embedded steel bars must be different from Eqs. (1) and (2), since stiffness provided by the external bars in the normal direction of the interface is different from the stiffness provided by embedded bars.

The present work intends to make a contribution to the current state-of-the-art of aggregate interlock modelling so the aforementioned limitations can be partially overcome. With that aim, an enhanced finite element model (FEM) is conceived in order to calibrate constitutive relations for aggregate interlock of a cracked concrete interface crossed by embedded steel bars and subjected to monotonic shear loading. Firstly, new constitutive relations are proposed for a crack in monolithic concrete. Then, the analysis focuses on the case of a cracked interface between concretes cast at different times (i.e. a free surface left without further treatment after vibration) (Mattock 1976). This latter type of interface is particularly common in connections between precast concrete elements (Tadros et al. 1993), in connections between precast elements and cast-in-place concrete (FIP

1982) and in structural rehabilitation and strengthening (Silfwerbrand 2003).

## 2 FEM for a Cracked Concrete Interface

In this section, a FE modelling approach for the analysis of a cracked (and reinforced) interface between concretes cast at different times (concrete joint) is presented. The 2D Fixed Bed (FB) approach introduced in Figueira et al. (2018) to simulate the behaviour of the dowel mechanism is used. That 2D FB approach is a discrete representation of a reinforcing bar dowel mechanism and in this paper is upgraded in order to model the other strength mechanisms (besides dowel action) of concrete interfaces. Thus, the following strength mechanisms are added to the model: bond-slip at the reinforcement/concrete interface and aggregate interlock.

The improved model is depicted in Fig. 1 and includes: (i) a steel reinforcing bar (nodes A and nodes B); (ii) a concrete substrate composed by two rigid blocks, one for the old concrete (nodes O) and the other for the new concrete (nodes N); (iii) steel/concrete interface FE's (connecting nodes A to nodes O and nodes B to nodes N) to simulate the deformability of the concrete substrate in the vicinity of the reinforcing bar; and (iv) a concrete interface FE (connecting node 1O to node 1 N) to simulate the aggregate interlock mechanism between the old concrete and the new concrete.

So the interpretation of the FE model configuration can be easier, Fig. 1 does not represent the true coordinates of the nodes in the model. In the model, nodes A coincide with nodes O, nodes B coincide with nodes N and consequently node 1O coincides with node 1 N.

### 2.1 Steel Reinforcing Bar

The steel reinforcing bar has a circular section and is discretized with fully numerically integrated Mindlin beam (class-III) (TNO DIANA 2014) FE's, including shear deformation effects. Each element has a length of 8 mm, 3 nodes, 2 Gauss integration points along its axis and 24 over its cross-section. The cross-section is integrated with a 6-point trapezoidal rule in the tangential direction and a 4-point Gauss scheme in the radial direction.

Other parameters of the reinforcing bar, as the total length, the bar diameter and the stress-strain constitutive relation are adapted to match a specific experimental test considered in the calibration of the FEM. The calibration is carried out comparing the shear stress obtained in the FEM with the shear stress measured in the experimental tests.

### 2.2 Concrete Substrate

The interface slip  $s$  and crack opening  $w$  are simulated by imposing those displacements to the nodes O belonging

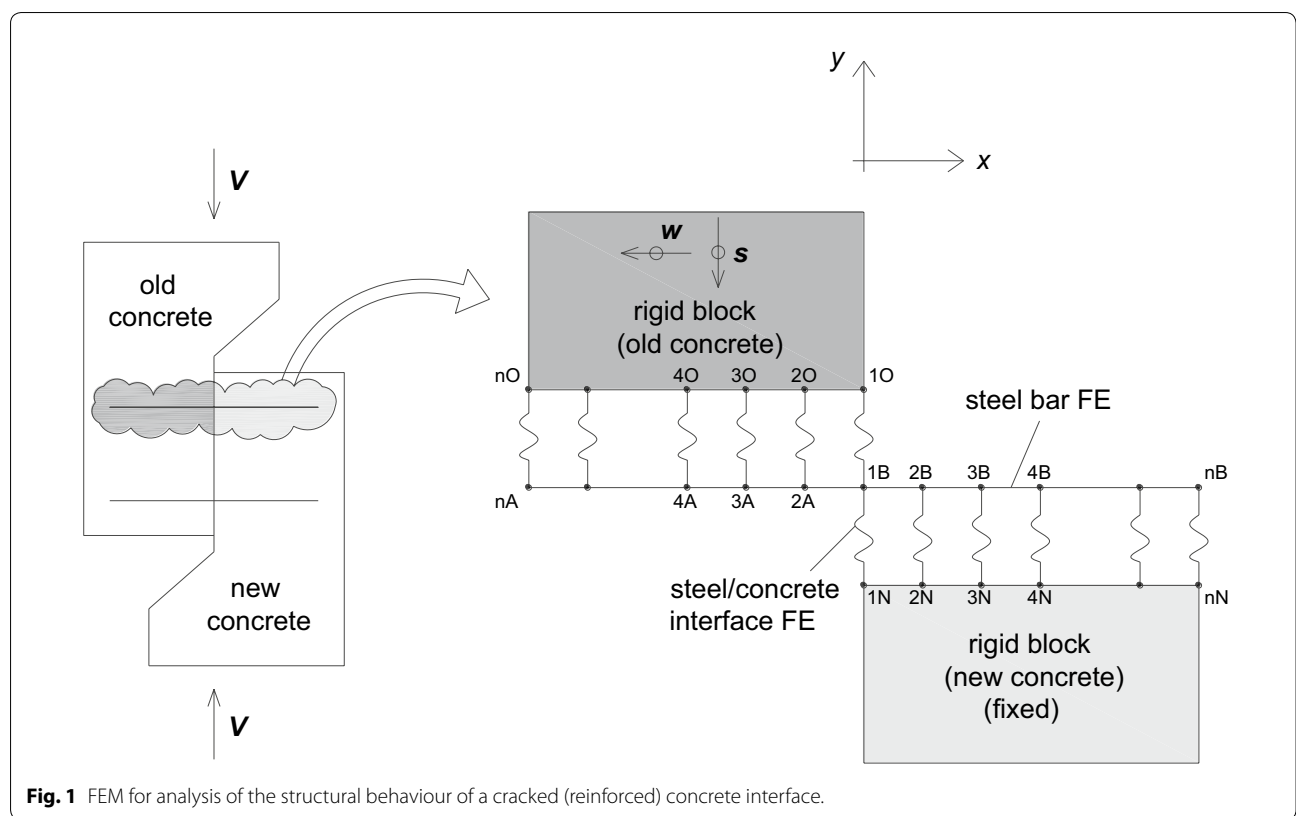


**Fig. 1** FEM for analysis of the structural behaviour of a cracked (reinforced) concrete interface.

to the old concrete rigid block (see Fig. 1), while the nodes N belonging to the new concrete rigid block remain fixed. In this context, the slip and crack opening values inserted in the FEM analyses will match the measured values in the experimental tests considered.

### 2.3 Steel/Concrete Interface

Each of the steel/concrete interface FE's reproducing the deformability of the concrete substrate surrounding the reinforcement is composed by two non-linear springs: one in the  $x$  direction (see Fig. 1) only to simulate the reinforcement bond slip mechanism; and the other in the  $y$  direction only to simulate reinforcement dowel action (Winkler spring). The steel/concrete interface FE's have a 4 mm spacing, which is equal to the reinforcing bar node spacing.

#### 2.3.1 Bond Slip

The bond slip mechanism of the reinforcement is considered by including in the FEM two-node, translation, non-linear, spring elements linking the steel bar to the concrete rigid blocks in the  $x$  direction (see Fig. 1). With the inclusion of those springs, interface crack opening originates bond stresses  $\tau_b$  along the bar surface. Consequently, an axial force is induced in the reinforcement.

The adopted constitutive model for the bond behaviour in each spring is the “tension chord model” of Martí et al. (1998), in which the  $\tau_b - \delta_x$  relation follows a perfectly plastic branch.  $\delta_x$  is the relative displacement in the  $x$  direction between the reinforcement and the concrete rigid blocks. Therefore, crack opening  $w$  is equal to the sum of  $\delta_x$  in the two concretes ( $\delta_{x,old} + \delta_{x,new}$ ) at the interface crack section ( $x=0$ ). For the bond stress  $\tau_b$ , the “tension chord model” assumes it as  $\tau_b = 2f_{ct}$ , in which  $f_{ct}$  is the concrete tensile strength. After reinforcement yielding, the spring perfectly plastic behaviour remains but the bond stress  $\tau_b$  is halved. In the present study, when information about  $f_{ct}$  of a specific experimental test is not available,  $f_{ct}$  is calculated through the fib Model Code expressions (fédération internationale du béton 2013) based on the concrete compressive strength.

#### 2.3.2 Dowel Action

The dowel action of the reinforcement is considered in the FEM similarly to the bond slip mechanism. The difference relies on the fact that the springs simulating dowel action work in the  $y$  direction (see Fig. 1). For dowel action, the Winkler spring constitutive relation considered in this study is the one presented in Figueira et al. (2018), which was calibrated to the experimental

tests of Dei Poli et al. (1992). The constitutive relation is nonlinear and written as:

$$dF_y = k_{sp} d\delta_y \quad (3)$$

where  $F_y$  is the spring force in the  $y$  direction,  $k_{sp}$  the spring stiffness for dowel action and  $\delta_y$  the relative displacement in the  $y$  direction between the reinforcement and the concrete rigid blocks. In turn,  $k_{sp}$  is given by:

$$k_{sp} = \psi(\delta_y, \phi, f_c) k_{0^*} \quad (4)$$

in which  $\psi$  is a nonlinearity coefficient (depending on  $\delta_y$ , the bar diameter  $\phi$  and the concrete compressive strength  $f_c$ ) and  $k_{0^*}$  the spring elastic stiffness for dowel action. These two parameters are expressed through the following equations:

$$\left\{ \begin{array}{l} \psi = 0.0116f_c + 0.4261 \Leftarrow \frac{\delta_y}{\phi} < 0.0065 \\ \psi = (-1.068f_c - 13) \left( \frac{\delta_y}{\phi} \right) + 0.02275f_c + 0.267 \Leftarrow 0.0065 \leq \frac{\delta_y}{\phi} \leq 0.022 \\ \psi = -0.00184f_c + 0.0825 \Leftarrow 0.022 < \frac{\delta_y}{\phi} < 0.117 \\ \psi = 0 \Leftarrow \frac{\delta_y}{\phi} \geq 0.117 \end{array} \right. \quad (5)$$

and

$$k_{0^*} = \frac{700 f_c^{0.7}}{\phi} \quad (6)$$

Finally, the influence of reinforcement kinking (geometric effect) in a concrete interface is also considered, so that the model accuracy is improved and the influence of this effect can be quantified and understood. For this purpose, geometric nonlinearity is activated through a classic Total Lagrange formulation, whose background theory is available in detail in TNO DIANA (2014).

## 2.4 Concrete Interface

The aggregate interlock mechanism is simulated, in the FEM, through a single concrete interface FE which connects node 1O to node 1 N (see Fig. 1). Two different approaches were followed in this paper to study the aggregate interlock effect:

- In some of the analyses, the constitutive model to describe the aggregate interlock behaviour was defined beforehand—this constitutive model expresses the normal and tangential stresses in the concrete interface FE as a function of the relative displacement between the connected nodes in the nor-

mal and tangential direction. The modelling approach described in the previous paragraph (inclusion of an interface FE to model the aggregate interlock effect) was used only in this situation.

- In the other approach, the constitutive model to describe the aggregate interlock effect was not known beforehand and the purpose of the analysis is precisely the quantification of the stresses transferred between concrete blocks through the aggregate interlock mechanism. This job is performed with the FEM illustrated in Fig. 1 containing the reinforcing bar, the concrete rigid blocks and the steel/concrete interface FE's, but without the concrete interface FE. In this case, the transferred stresses are calculated as the sum of the reactions in the nodes corresponding to one concrete rigid block divided by the area of the concrete interface.

Regarding the analyses with an interface FE, an additional remark must be made. The employed constitutive models to describe the aggregate interlock effect are different from the ones already available in the used FE package (TNO DIANA BV 2014). Therefore, a user-supplied subroutine was utilized to input the new constitutive models in the FE analyses. User-supplied subroutines are a useful feature of the TNO DIANA software which allow the programming of user-defined constitutive models to be used in the nonlinear analyses.

### 2.4.1 Constitutive Relation in the Interface Tangential Direction

As was mentioned in Sect. 1 on the study implemented by Feenstra et al. (1991a, b), it was concluded that Walraven and Reinhardt (1981) formulation, among other available alternatives, has the best behaviour in terms of the stability of the numerical solution. For that reason, when cracks in monolithic concrete are studied, Eq. (1) is considered, at first place in this work, to define the constitutive model for the interface FE in terms of shear stress (stress in the tangential direction—direction  $y$  in Fig. 1).

When new constitutive relations need to be determined, the adopted shape for those relations are

modified versions of Eq. (1) obtained through the introduction of new coefficients such that:

$$\tau_{\text{agg,FEM}} = C_f \{ a_1 f_{cc} + [b_1 w^{c_1} + (d_1 w^{e_1} + f_1) f_{cc}] s \} \quad (7)$$

or

$$V_{\text{agg,FEM}} = C_f \{ a_1 f_{cc} + [b_1 w^{c_1} + (d_1 w^{e_1} + f_1) f_{cc}] s \} b L \quad (8)$$

in which coefficients  $C_f$  to  $f_1$  are calculated through the Nonlinear Generalized Reduced Gradient optimization algorithm of Lasdon et al. (1978). The automatic implementation of this algorithm is included in the Microsoft Excel Solver tool and its background theory can be consulted in detail in Coello et al. (2007). The coefficients  $C_f$  to  $f_1$  are calculated aiming to minimize the difference  $d$

$$d = |V - V_{\text{FEM}}| \quad (9)$$

In Eq. (9),  $V$  is the shear force measured in experimental tests and  $V_{\text{FEM}}$  is the calculation result, given by the sum of  $V_{\text{agg,FEM}}$  calculated in Eq. (8) and the dowel force  $V_{\text{d,FEM}}$  obtained in the FEM illustrated in Fig. 1:

$$V_{\text{FEM}} = V_{\text{agg,FEM}} + n V_{\text{d,FEM}} \quad (10)$$

where  $n$  is the number of bars crossing the interface.

It is important to note that this optimization problem is indeterminate, since different sets of coefficients can lead to similar results in terms of the difference  $d$ . Therefore, the determination of the coefficient values was made keeping the coefficient values presented in Eq. (1) whenever possible. Whenever possible as well, only the coefficient  $C_f$  was considered as a variable. More details on this process are given in Sect. 4.2.

#### 2.4.2 Constitutive Relation in the Interface Normal Direction

The relationship given by Eq. (2) was derived from tests in which the interface crack opening is restrained by external and unbonded reinforcing bars. The stiffness of such a confining system can be significantly different from the one provided by embedded reinforcing bars. Therefore, it is not surprising that Eq. (2) does not provide an accurate representation of the normal stress in interfaces crossed by embedded bars, such as the ones studied in the present paper. In this work, the actual normal stress at the interface is calculated in analyses according to the approach illustrated in Fig. 1. It is therefore given by:

$$\sigma_n = \frac{n F_{s,x}}{b L} \quad (11)$$

Consequently, the corresponding normal force at the interface is:

$$N = n F_{s,x} \quad (12)$$

where  $F_{s,x}$  is the bar force component at the interface section ( $x=0$ ) in the  $x$  axis direction (see Fig. 1).

### 3 Review and Selection of Experimental Data for Calibration of Aggregate Interlock Constitutive Models

In order to select the tests suitable to be compared with results provided by the FEMs for concrete interfaces, a review of the experimental data available in the literature was made. Firstly, the discussion focuses on tests which were performed to analyse (experimentally) dowel action as the only strength mechanism. Then, the case of dowel action interacting with aggregate interlock in monolithic concrete cracks is reviewed. Finally, the case of dowel action interacting with aggregate interlock in an interface between concretes cast at different times is brought into focus.

#### 3.1 Dowel Action as the Only Strength Mechanism

Figueira et al. (2018) contains an extensive review on experimental tests devised to study the dowel action mechanism. It was concluded in that work that the experimental assessment of dowel action in a reinforced concrete interface is a complex task, since the conception of a specimen execution procedure that can eliminate the influence of other strength mechanisms is hard to accomplish. In this context, due to the reasons explained in Figueira et al. (2018), only the tests of Dei Poli et al. (1992) should be considered for the calibration of a dowel action FEM.

#### 3.2 Cracks in Monolithic Concrete

A large collection of experimental data referring to cracks in monolithic concrete subjected to monotonic shear loading can be found in Figueira et al. (2016). In this present paper, only campaigns containing data about the  $V-s$  (shear force–slip) and  $s-w$  interface measurements are considered, since that information is crucial for the calibration of a nonlinear FEM. Those campaigns are the ones of Mansur et al. (2008), Mattock (1976) and Walraven and Reinhardt (1981). However, some aspects observed in the results of the first two led to put them apart:

- In the Mansur et al. (2008) tests, slip values at the maximum force were around 3 mm, while the average value of several tests available in literature (Hofbeck et al. 1969; Mattock 1976; Walraven and Rein-

hardt 1981) with the same characteristics is around 0.5 to 0.6 mm. For the fact, no reason is identified in Mansur et al. (2008).

- In the Mattcock (1976) program, interface slip and crack opening measurements revealed that the transducers used, during an important part of the tests, did not appear to have the desired accuracy. For that reason, the measured crack opening values were significantly lower than the order of magnitude that can be expected for this type of structure. Consequently, their consideration in the constitutive relations for aggregate interlock would lead to unrealistic stress values.

Therefore, the Walraven and Reinhardt (1981) campaign will be taken as a reference hereinafter in this paper for FE modelling of the shear behaviour of a crack in reinforced monolithic concrete. Regarding this experimental program, some notes are relevant:

- As was pointed out in Figueira et al. (2016), when reinforcement ratio,  $\rho$ , is high ( $\rho f_y/f_c > 0.25$ , where  $f_c$  is the concrete compressive strength and  $f_y$  is the reinforcement yield stress), secondary cracks occur and consequently the structure behaviour cannot be represented through the modelling approach used in this paper. For that reason, tests in which  $\rho f_y/f_c > 0.25$  will not be considered in the present calibration.
- For the assessment of concrete compressive strength, only cubic specimens were tested. In the aggregate

interlock relations of Eqs. (1) and (2), that value  $f_{cc}$  is considered. But for the dowel action and bond models the concrete compressive strength in cylinders is needed. That strength value is hereinafter estimated as  $f_c = 0.85 f_{cc}$ .

The properties of the 7 specimens considered, as well as their shear strength, are shown in Table 1 where:  $b$  is the interface width,  $L$  the interface length,  $\phi$  the reinforcing bar diameter,  $c$  the lateral concrete cover and  $V_R$  the shear strength.

### 3.3 Interfaces Between Concretes Cast at Different Times

Three roughness profiles are commonly adopted for interfaces between concretes cast at different times: intentionally roughened surface, free surface (left without treatment after vibration of the old concrete) and smooth surface (i.e., a surface cast against steel, plastic or specially prepared wooden moulds). Data available in literature for each roughness type is scarce and in this context the same criteria stated for the case of monolithic concrete cracks are adopted for interfaces between concretes cast at different times. As a result, the tests considered are only the 3 (M1, M2 and M3) performed in Figueira et al. (2015), which correspond to free surfaces. Table 2 summarizes the specimen properties and the shear strength values measured, where  $f_{c1}$  is the compressive strength of the old concrete and  $f_{c2}$  the compressive strength of the new concrete.

**Table 1 Experimental data for shear strength of reinforced monolithic concrete cracks collected from the Walraven and Reinhardt (1981) experimental program.**

Test	$b$ (mm)	$L$ (mm)	$f_c$ (MPa)	$f_y$ (MPa)	$\rho$ (%)	$\phi$ (mm)	$V_R$ (kN)
240208	120	300	16.9	460	0.56	8	167.4
110208	120	300	26.1	460	0.56	8	198.8
110408	120	300	26.1	460	1.12	8	231.8
230208	120	300	47.7	460	0.56	8	241.9
230408	120	300	47.7	460	1.12	8	389.9
230608	120	300	47.7	460	1.68	8	452.2
230808	120	300	47.7	460	2.23	8	510.8

**Table 2 Experimental data for shear strength of reinforced interfaces between concretes cast at different times collected from the tests performed in Figueira et al. (2015).**

Test	$b$ (mm)	$L$ (mm)	$f_{c1}$ (MPa)	$f_{c2}$ (MPa)	$f_y$ (MPa)	$\rho$ (%)	$\phi$ (mm)	$V_R$ (kN)
M1	150	250	67.8	48.1	605	1.07	8	202.2
M2	150	250	67.8	48.1	605	1.07	8	196.2
M3	150	250	67.8	48.1	605	1.07	8	201.3

## 4 Calibration of Aggregate Interlock Constitutive Models for Cracks in Monolithic Concrete

Once a detailed FEM methodology is available for calculating the contribution of the dowel action mechanism, the aggregate interlock effect in the experimental tests considered in this work can be isolated and determined. Besides the influence of parameters as the concrete strength, steel yield stress and reinforcement ratio, shear transfer by aggregate interlock largely depends on the interface roughness. Therefore, different constitutive relations should be defined for cracks in monolithic concrete compared to cracks in concrete joints.

### 4.1 First Analysis Using the Constitutive Relation of Walraven and Reinhardt

In a first analysis, Eq. (1) with  $C_f = 1$  was considered for shear transfer by aggregate interlock in the tangential interface direction. The calculation output showed that the experimental shear strength values  $V_R$  are significantly higher than the strength  $V_{R,FEM,1}$  achieved in this FE first analysis (see Fig. 2a). These results are summarized in Table 3, where the relation  $V_R/V_{R,FEM,1}$  has an average value of  $\mu = 1.31$  and standard deviation  $\sigma = 0.15$ . This difference between  $V_R$  and  $V_{R,FEM,1}$  notably increases with the concrete strength. It also increases with reinforcement ratio, but more slightly.

In terms of dowel forces, the contribution to interface shear transfer is residual, varying from 7.2% in specimen 110208 to 16.4% in specimen 230808 (see Fig. 9b).

The discrepancy between these experimental measurements and the FEM outcome is evident and can be attributed to the fact that Eq. (1) is not valid in this case. It should be remembered that the equation was fitted to the results of tests in specimens without embedded reinforcement. The steel/concrete bond increases stiffness in the normal direction of the interface and, consequently, shear strength as well. In order to include this phenomenon in the FEM, a second analysis is implemented.

### 4.2 Second Analysis with an Improved Constitutive Relation for Aggregate Interlock

Different possibilities for the new improvements in Eq. (1) were tested in this second analysis. It was concluded that the discrepancy between the experimental measurements and the FEM results mainly occurs in the shear strength values. Thus, a change in the coefficient  $C_f$  should be considered at first place, with the inclusion of the main parameters interacting in the bond mechanism: concrete strength and reinforcement ratio. In this context, it was mentioned before that the concrete strength has a bigger influence on the difference between  $V_R$  and  $V_{R,FEM,1}$  than the reinforcement ratio. To take this fact

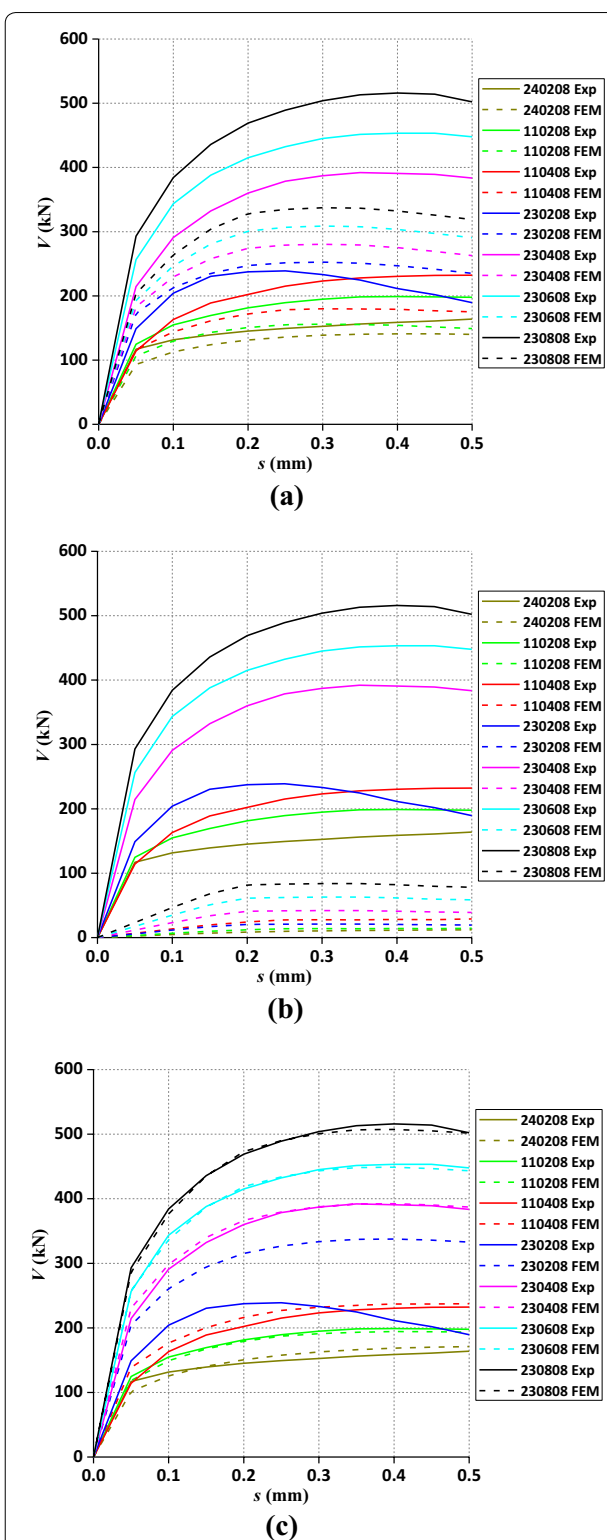


**Fig. 2** Comparison of Walraven and Reinhardt (1981) experimental tests with FEM results: **a** first analysis considering Eq. (1); **b** values for reinforcement dowel action; **c** second analysis considering an improved constitutive relation for aggregate interlock.

**Table 3 Comparison of Walraven and Reinhardt (1981) experimental values with FEM results obtained in the two analyses implemented: 1— $V_{\text{FEM}}$  considering Eq. (1); 2— $V_{\text{FEM}}$  considering the improved constitutive relation for aggregate interlock.**

Test	$V_R$ (kN)	$V_{R,\text{FEM},1}$ (kN)	$V_R/V_{R,\text{FEM},1}$	$V_{dR,\text{FEM}}$ (kN)	$V_{dR,\text{FEM}}/V_R$	$V_{R,\text{FEM},2}$ (kN)	$V_R/V_{R,\text{FEM},2}$
240208	167.4	140.9	1.19	12.09	0.072	171.1	0.98
110208	198.8	156.1	1.27	14.48	0.073	194.4	1.02
110408	231.8	180.0	1.29	28.95	0.125	237.4	0.98
230208	241.9	231.7	1.04	20.98	0.087	337.5	0.72
230408	389.9	280.5	1.39	41.96	0.108	392.3	0.99
230608	452.2	308.7	1.46	62.94	0.139	448.3	1.01
230808	510.8	337.3	1.51	83.91	0.164	507.5	1.01
	$\mu$	1.31					0.96
	$\sigma$	0.15					0.10

into consideration, the contribution of the two parameters were separated and the following expression for the new coefficient  $C_f^*$  was reached:

$$C_f^* = 1 + a_2 f_{cc} + b_2 \rho \quad (13)$$

where  $a_2$  and  $b_2$  are coefficients determined through optimization algorithms (Coello Coello et al. 2007; Lasdon et al. 1978) in order to approximate  $V_{R,\text{FEM}}$  to  $V_R$ . For that purpose, a good experimental data basis is available in the tests of Walraven and Reinhardt (1981) (see Table 1), since four reinforcement ratios (0.56%, 1.12%, 1.68% and 2.23%) and three concrete strengths (16.9 MPa, 26.1 MPa and 47.7 MPa) were considered for the specimens. The values attained for the coefficients  $a_2$  and  $b_2$  were:

$$a_2 = 0.00422$$

$$b_2 = 18.2$$

Figure 3 presents values of the new coefficient  $C_f^*$  calculated from Eq. (13) and significantly higher values are obtained compared to the coefficient  $C_f$  of Eq. (1), where  $C_f$  should be taken as 0.35 if the crack crosses the aggregates and 1.0 otherwise.

Additionally, it was also concluded that additional improvements could be made in the aggregate interlock model in order to fit the experimental behaviour. A much better adjustment to the experimental results was achieved with new values for the coefficients  $e_1$  and  $f_1$  expressed in Eq. (7). Instead of  $e_1 = -0.707$  and  $f_1 = -0.20$ , these new values are proposed:

$$e_1 = -0.673$$

$$f_1 = -0.17$$

Then, aggregate interlock contribution in a monolithic concrete crack with reinforcing bars can be calculated as:

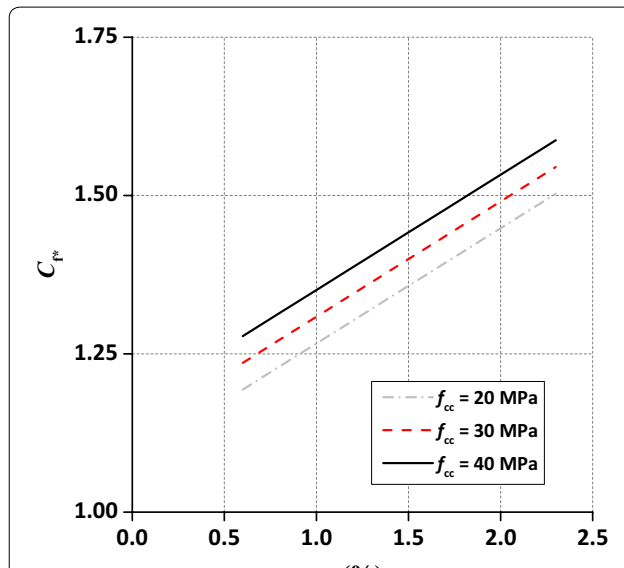


**Fig. 3** Values of the new coefficient  $C_f^*$  depending on the concrete strength and the reinforcement ratio.

$$\tau_{\text{agg}} = C_f^* \left\{ -0.0333 f_{cc} + \left[ 1.8 w^{-0.8} + (0.234 w^{-0.673} - 0.17) f_{cc} \right] s \right\} \quad (14)$$

The improvements achieved with these new coefficients are represented in Fig. 2c and in Table 3, where  $V_{R,\text{FEM},2}$  is the shear strength obtained in the FEM for this second analysis. Now, the relation  $V_R/V_{R,\text{FEM},2}$  has an average value of  $\mu = 0.96$  and standard deviation  $\sigma = 0.10$ .

It can be noticed in the results that specimen 230208 diverges from all the others, having  $V_{R,\text{FEM},2}$  significantly higher than  $V_R$ . In this case, the difference between the two values occurs because the ratio  $(\rho f_y)/f_c$  for the test is equal to 0.054 and consequently

very low. In Figueira et al. (2016), it was mentioned that when  $(\rho f_y)/f_c < 0.075$ , approximately, normal stress on the interface is not enough to cause plasticity in the compressed contact areas between the two concretes. Therefore, the cohesion mechanism is not

mobilized and aggregate interlock is only provided by shear friction. Since the aggregate interlock behaviour is different in these situations, Eq. (14) and the new coefficients  $e_1$  and  $f_1$  should apply exclusively when  $0.075 < (\rho f_y)/f_c < 0.25$ . For  $(\rho f_y)/f_c < 0.075$ , the conception of an aggregate interlock modelling approach requires more experimental data than just one single test.

Furthermore, it is important to mention that Eq. (1) was calibrated by Walraven and Reinhardt (1981) for slip values up to 2.5 mm in tests on cracks in monolithic concrete restrained by external bars. In the tests on cracks with embedded bars only slip values up to 0.5 mm are available. The new coefficients of Eq. (14) were calibrated for the interface response in that range. Nevertheless, the stress softening behaviour implicit in Eq. (1) for large slip values is maintained in Eq. (14), as is depicted in Fig. 4 referring to test 230808 (see Table 1).

Figure 5a presents  $\tau_{agg}$ - $s$  graphs calculated from Eq. (14) for several crack opening values, with  $C_f = 1.64$  and  $f_{cc} = 56.1$  MPa corresponding to test 230808 (see Table 1). The same type of graphs is shown in Fig. 5b with  $\tau_{agg}$  calculated from Eq. (1), in which  $C_f = 1$  and  $f_{cc} = 56.1$  MPa. As can be seen, the linear response observed in the Eq. (1) graphs is conserved when the new coefficients are introduced. Differences are mainly detected in the fact that Eq. (14) provides higher values for  $\tau_{agg}$ .

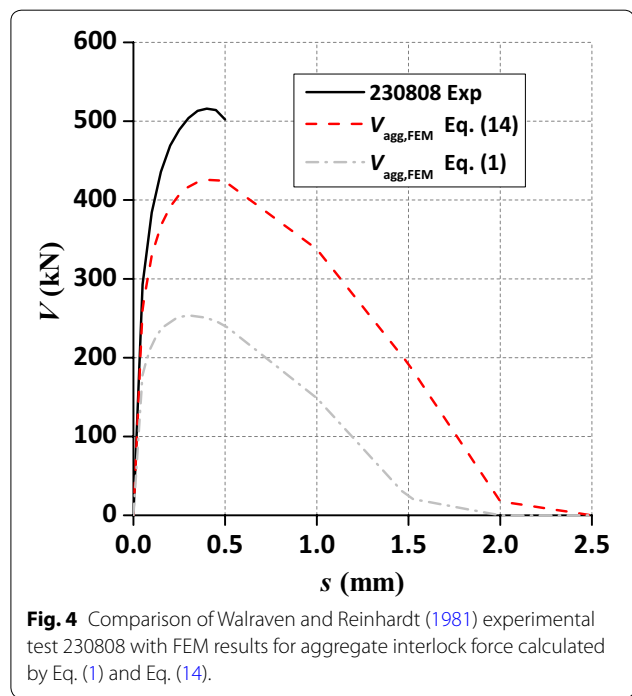


**Fig. 4** Comparison of Walraven and Reinhardt (1981) experimental test 230808 with FEM results for aggregate interlock force calculated by Eq. (1) and Eq. (14).

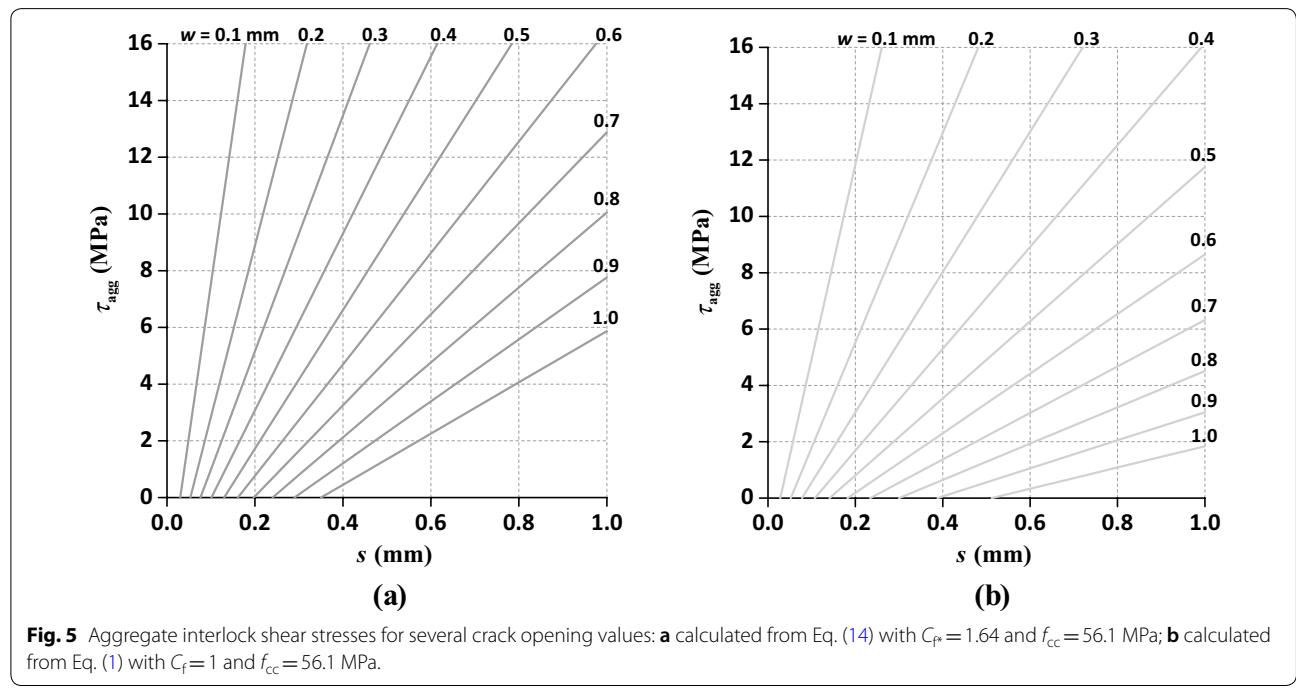


**Fig. 5** Aggregate interlock shear stresses for several crack opening values: **a** calculated from Eq. (14) with  $C_f = 1.64$  and  $f_{cc} = 56.1$  MPa; **b** calculated from Eq. (1) with  $C_f = 1$  and  $f_{cc} = 56.1$  MPa.

## 5 Calibration of Aggregate Interlock Constitutive Models for an Interface Between Concretes Cast at Different Times

In this section, aggregate interlock constitutive relations are derived for cracked (and reinforced) interfaces between concretes cast at different times whose roughness profile corresponds to a free surface (left without treatment after vibration of the old concrete). Concerning the intentionally roughened surfaces, their strength and behaviour is close to what is observed in monolithic concrete cracks (Figueira et al. 2016; Mattock 2001). Furthermore, a similar strength and behaviour can also be identified between the smooth surfaces and the free surfaces (Figueira et al. 2015; Mattock 1976).

Since a significant influence of the reinforcement dowel action is expected for the shear transfer in interfaces between concretes cast at different times, the dowel action behaviour obtained in the FEM is first presented and discussed. Then, the aggregate interlock contribution is assessed and the constitutive model is calibrated from the experimental results available.

### 5.1 Dowel Action Contribution

The dowel action contribution obtained in the FEM for the shear transfer in an interface between concretes cast at different times is illustrated in Fig. 6 (red curve), where the average experimental response of specimens M1, M2 and M3 (see Table 2) is also included (black curve). It can be noticed and confirmed that dowel action weight in the total experimental shear force is much more substantial

in comparison with cracks in monolithic concrete. At the peak experimental shear force ( $V=199.9$  kN), dowel contribution ( $V_{d,FEM}=84.38$  kN) represents 42.2%. This influence increases with slip until a maximum ( $\approx 82\%$ ) is reached for very large displacements ( $s>6.6$  mm), where structural serviceability limits are already exceeded. The continuous growth of the dowel force with slip is caused by the geometric or kinking effect of the reinforcing bars.

The influence of interface crack opening and the kinking effect of a reinforcing bar can be seen more clearly in Fig. 7, which reveals the dowel force–slip response obtained in the FEM for three different configurations or hypotheses: (i) interface with no crack opening; (ii) interface with crack opening; and (iii) interface with crack opening and the kinking effect activated. At the beginning of the imposed displacements, no differences between the three hypotheses are observed. As the slip grows, the reinforcing bar of the specimen with crack opening yields first ( $s \approx 0.4$  mm) and the resulting dowel force has lower values. With the reinforcement yielding and the formation of a plastic hinge, the rotation of the reinforcement axis at the intersection with the interface starts to be significant. Then, the kinking effect starts to manifest its influence, which grows continuously with the slip increasing. For very large displacements, most of the Winkler springs enter the residual force branch and the reinforcement curvatures and displacements cease to alter the mobilized dowel force. Thus, crack opening influence fades away at that stage.

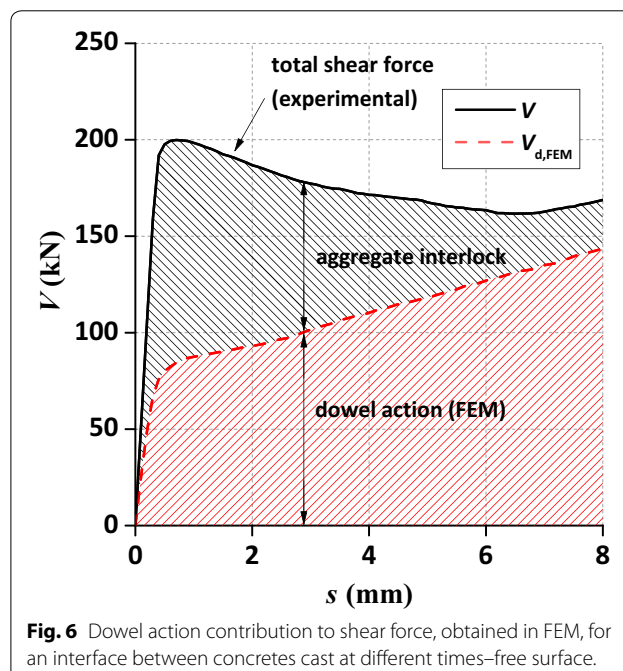


**Fig. 6** Dowel action contribution to shear force, obtained in FEM, for an interface between concretes cast at different times–free surface.

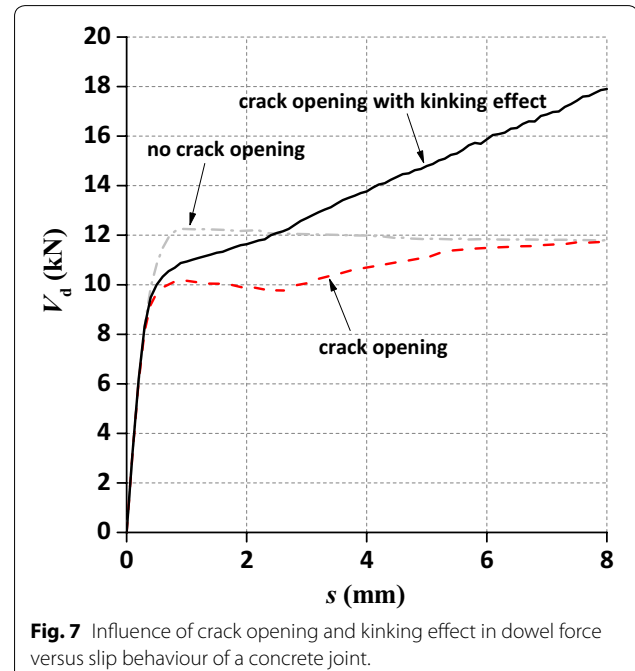
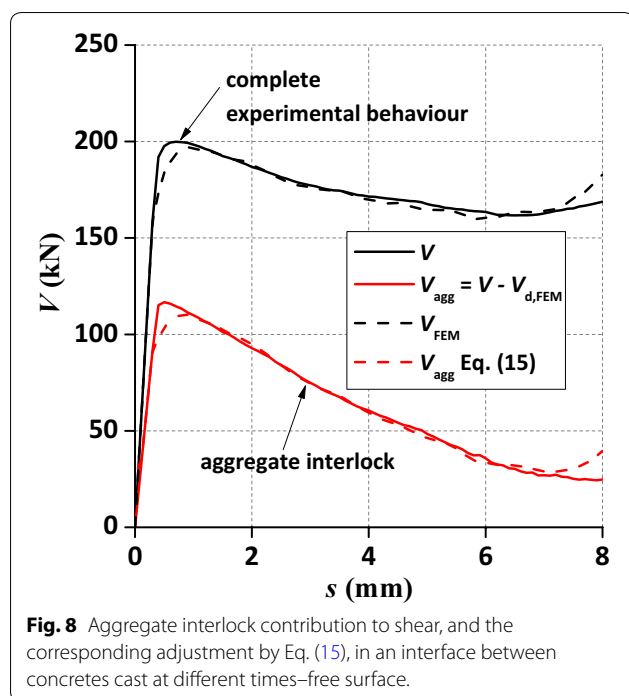


**Fig. 7** Influence of crack opening and kinking effect in dowel force versus slip behaviour of a concrete joint.



calculated in the FEM. It can be observed that the maximum shear force  $V_{\text{agg}}$  for the aggregate interlock mechanism occurs at a low slip value ( $s=0.5 \text{ mm}$ ). Afterwards,  $V_{\text{agg}}$  decreases continuously along with the growth of slip and crack opening in the interface, until a residual value is achieved.

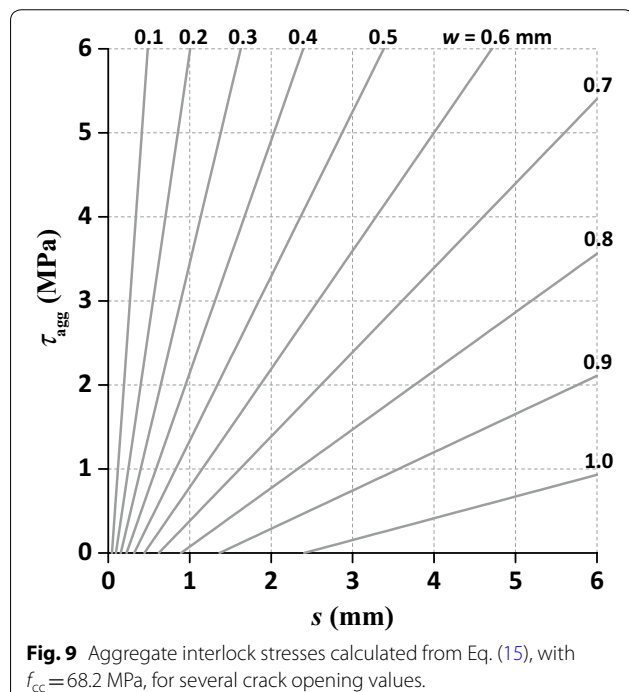
For interfaces with this type of roughness profile (free surface), new constitutive relations for shear transfer by aggregate interlock are formulated in the present work. During the formulation procedure, like the one implemented for cracks in monolithic concrete in the previous Sect. 4.2, it was verified that in order to get a very good fit, all coefficients from Eq. (14) should be altered. In this context, the expression that provides the best results is the following:

$$\tau_{\text{agg}} = 0.058 \times \left\{ -0.157f_{cc} + [2.753w^{-0.524} + (0.478w^{-0.896} - 0.453)f_{cc}]s \right\} \quad (15)$$

where  $f_{cc}$  is the average value between the two concretes of the compressive strength measured in cubic specimens.

Figure 8 also shows the values calculated from Eq. (15) and a very good adjustment is achieved until  $s=7 \text{ mm}$ , approximately. However, it is important to refer that Eq. (15) is calibrated for a single set of parameters interfering in aggregate interlock mobilization corresponding to tests M1, M2 and M3: average concrete strength  $f_c=58.0 \text{ MPa}$  and  $\rho \times f_y=6.47 \text{ MPa}$ . These values were defined to represent the typical case of an interface between a precast beam and the cast-in-place slab of a concrete bridge. For a specimen with properties that differ significantly from these, a new calibration for the coefficients of Eq. (15) is recommended using the same procedure.

Finally,  $\tau_{\text{agg}}-s$  graphs calculated from Eq. (15) for several crack opening values can be seen in Fig. 9, with  $f_{cc}=58.0/0.85=68.2 \text{ MPa}$  corresponding to the M1, M2 and M3 tests. Comparing with Fig. 5 for cracks in monolithic concrete, a linear response is observed as well for free surfaces, since Eq. (15) also imposes that  $\tau_{\text{agg}}$  varies linearly with slip when crack opening is constant. However, besides a similar linear response, much lesser values are obtained for  $\tau_{\text{agg}}$  in free surfaces compared to the cracks in monolithic concrete.



## 5.2 Constitutive Model for Aggregate Interlock

Figure 8 presents the aggregate interlock contribution, which is obtained from the difference between the experimentally measured shear force on the concrete joint (Figueira et al. 2015) and the dowel action force

## 6 Conclusions

In this paper, the following conclusions were reached:

1. A FEM for the case of a concrete joint with embedded reinforcing bars, subjected to slip and crack opening displacements, was formulated and

- achieved. Dowel action modelling conceived in Figueira et al. (2018) was extended for the purpose. Bond between the steel bars and the surrounding concrete was considered and an interface FE was included to simulate aggregate interlock.
2. Changes were introduced in the aggregate interlock empirical constitutive relations available in the literature for cracks in monolithic concrete restrained by external bars. The modifications were implemented in order to include the contribution of the steel/concrete bond. With this upgrade, the ratio between the experimental and the FEM values ( $V_R/V_{R,FEM}$ ) was significantly improved, from an average value of  $V_R/V_{R,FEM} = 1.36$  to  $V_R/V_{R,FEM} = 0.96$ . The constitutive relations derived are applicable to the case of an interface with embedded bars (in the range  $0.075 < (\rho f_y)/f_c < 0.25$ ) and can effectively predict the stress-displacement behaviour observed in the experimental tests on those interfaces.
  3. New constitutive relations were also proposed for shear transfer by aggregate interlock in a concrete joint, whose roughness profile corresponds to a free surface (left without treatment after vibration). The expressions were calibrated for a single set of parameters interacting in aggregate interlock mobilization: average concrete strength  $f_c = 58.0$  MPa and  $\rho f_y = 6.47$  MPa. For specimens with properties that differ significantly from these, a new calibration for the constitutive relations is recommended using the same procedure.

#### Acknowledgements

The authors gratefully acknowledge the support provided by LEMC-Laboratório de Ensaio de Materiais de Construção.

#### Authors' contributions

DF carried out the literature review; conceived, designed and performed some of the experimental tests considered in this study, and the FEM numerical analyses; participated in the discussion of the results obtained and the conclusions; wrote the manuscript. CS cooperated with DF throughout the study as co-author in all the tasks. ASN supervised and reviewed all stages and tasks of the work, contributing actively in the discussion of the results and conclusions. All authors read and approved the final manuscript.

#### Funding

This work was financially supported by: UID/ECI/04708/2019–CONSTRUCT–Institute of R&D in Structures and Construction funded by national funds through the FCT/MCTES (PIDDAC); Ph.D. Grant SFRH/BD/65111/2009.

#### Availability of data and materials

Please contact corresponding author for data requests.

#### Competing interests

The authors declare that they have no competing interests.

#### Author details

<sup>1</sup> Faculty of Engineering & Informatics, University of Bradford, Bradford BD7 1DP, UK. <sup>2</sup> CONSTRUCT-LABEST, Faculty of Engineering (FEUP), University of Porto, Rua Dr. Roberto Frias, s/n, 4200-465 Porto, Portugal.

Received: 4 July 2019 Accepted: 31 December 2019  
Published online: 17 March 2020

#### References

- Bazant, Z. P., & Gambarova, P. G. (1980). Rough cracks in reinforced concrete. *ASCE Journal of the Structural Division*, 106(4), 819–842.
- Coello, C. A., Lamont, G. B., & Van Veldhuizen, D. A. (2007). *Evolutionary algorithms for solving multi-objective problems*. New York: Springer.
- Dei Poli, S., Di Prisco, M., & Gambarova, P. G. (1992). Shear response, deformations and subgrade stiffness of a dowel bar embedded in concrete. *ACI Structural Journal*, 89(6), 665–675.
- Dias-da-Costa, D., Alfaiate, J., & Júlio, E. N. B. S. (2012). FE modeling of the interfacial behaviour of composite concrete members. *Construction and Building Materials*, 26(1), 233–243.
- Espeche, A. D., & León, J. (2011). Estimation of bond strength envelopes for old-to-new concrete interfaces based on a cylinder splitting test. *Construction and Building Materials*, 25(3), 1222–1235.
- Fang, Z., Jiang, H., Liu, A., Feng, J., & Chen, Y. (2018). Horizontal shear behaviors of normal weight and lightweight concrete composite T-beams. *International Journal of Concrete Structures and Materials*, 12(1), 55.
- fédération internationale du béton. (2013). *fib model code for concrete structures 2010*. Berlin: Ernst & Sohn Publisher.
- Feenstra, P. H., de Borst, R., & Rots, J. G. (1991a). Numerical study on crack dilatancy. I: Models and stability analysis. *Journal of Engineering Mechanics*, 117(4), 733–753.
- Feenstra, P. H., de Borst, R., & Rots, J. G. (1991b). Numerical study on crack dilatancy. II: Applications. *Journal of Engineering Mechanics*, 117(4), 754–769.
- Figueira, D., Sousa, C., Calçada, R., & Serra Neves, A. (2015). Push-off tests in the study of the cyclic behavior of interfaces between concretes cast at different times. *Journal of Structural Engineering*, 142(1), 04015101.
- Figueira, D., Sousa, C., Calçada, R., & Serra Neves, A. (2016). Design recommendations for reinforced concrete interfaces based on statistical and probabilistic methods. *Structural Concrete*, 17(5), 811–823.
- Figueira, D., Sousa, C., & Serra Neves, A. (2018). Winkler spring behavior in FE analyses of dowel action in statically loaded RC cracks. *Computers and Concrete*, 21(5), 593–605.
- FIP. (1982). *Shear at the interface of precast and in situ concrete*. Lausanne: Fédération Internationale de la Precontrainte.
- Gambarova, P. G., & Karakoç, C. (1983). A new approach to the analysis of the confinement role in regularly cracked concrete elements. In *Transactions of the 7th International Conference on Structural Mechanics in Reactor Technology*, H5(7), 251–261.
- Haskett, M., Oehlers, D. J., Ali, M. M., & Sharma, S. K. (2011). Evaluating the shear-friction resistance across sliding planes in concrete. *Engineering Structures*, 33(4), 1357–1364.
- Hofbeck, J. A., Ibrahim, I. O., & Mattock, A. H. (1969). Shear transfer in reinforced concrete. *ACI Journal Proceedings*, 66(2), 119–128.
- Kim, Y.-J., Chin, W.-J., & Jeon, S.-J. (2018). Interface shear strength at joints of ultra-high performance concrete structures. *International Journal of Concrete Structures and Materials*, 12(1), 59.
- Kwan, A. K. H., & Ng, P. L. (2013). Modelling dowel action of discrete reinforcing bars for finite element analysis of concrete structures. *Computers and Concrete*, 12(1), 19–36.
- Lasdon, L. S., Waren, A. D., Jain, A., & Ratner, M. (1978). Design and testing of a generalized reduced gradient code for nonlinear programming. *ACM Transactions on Mathematical Software*, 4(1), 34–50.
- Li, B., Maekawa, K., & Okamura, H. (1989). Contact density model for stress transfer across cracks in concrete. *University of Tokyo Journal of the Faculty of Engineering*, 40(1), 9–52.
- Magliulo, G., Ercolino, M., Cimmino, M., Capozzi, V., & Manfredi, G. (2014). FEM analysis of the strength of RC beam-to-column dowel connections under monotonic actions. *Construction and Building Materials*, 69, 271–284.
- Mansur, M. A., Vinayagam, T., & Tan, K.-H. (2008). Shear transfer across a crack in reinforced high-strength. *Journal of Materials in Civil Engineering*, 20(4), 294–302.
- Marti, P., Alvarez, M., Kaufmann, W., & Sigrist, V. (1998). Tension chord model for structural concrete. *Structural Engineering International*, 8(4), 287–298.

- Mattock, A. H. (1976). *Shear transfer under monotonic loading across an interface between concretes cast at different times*. SM 76-3. Seattle: University of Washington.
- Mattock, A. H. (2001). Shear friction and high-strength concrete. *ACI Structural Journal*, 98(1), 50–59.
- Millard, S., & Johnson, R. (1984). Shear transfer across cracks in reinforced concrete due to aggregate interlock and dowel action. *Magazine of Concrete Research*, 36(126), 9–21.
- Mohamad, M. E., Ibrahim, I. S., Abdullah, R., Rahman, A. A., Kueh, A. B. H., & Usman, J. (2015). Friction and cohesion coefficients of composite concrete-to-concrete bond. *Cement & Concrete Composites*, 56, 1–14.
- Moradi, A. R., Soltani, M., & Tasnim, A. A. (2012). A simplified constitutive model for dowel action across RC cracks. *Journal of Advanced Concrete Technology*, 10(8), 264–277.
- Niwa, J., Matsumoto, K., Sato, Y., Yamada, M., & Yamauchi, T. (2016). Experimental study on shear behavior of the interface between old and new deck slabs. *Engineering Structures*, 126, 278–291.
- Paulay, T., & Loeber, P. J. (1974). Shear transfer by aggregate interlock. *ACI Special Publication*, 42, 1–16.
- Rahal, K. N., Khaleefi, A. L., & Al-Sanee, A. (2016). An experimental investigation of shear-transfer strength of normal and high strength self compacting concrete. *Engineering Structures*, 109, 16–25.
- Randl, N. (2007). Load bearing behaviour of cast-in shear dowels. *Beton-und Stahlbetonbau*, 102, 31–37.
- Randl, N. (2013). Design recommendations for interface shear transfer in fib Model Code 2010. *Structural Concrete*, 14(3), 230–241.
- Saldanha, R., Júlio, E., Dias-da-Costa, D., & Santos, P. (2013). A modified slant shear test designed to enforce adhesive failure. *Construction and Building Materials*, 41, 673–680.
- Santos, P. M., & Júlio, E. N. (2014). Interface shear transfer on composite concrete members. *ACI Structural Journal*, 111(1), 113–121.
- Silfwerbrand, J. (2003). Shear bond strength in repaired concrete structures. *Materials and Structures*, 36, 419–424.
- Tadros, M. K., Ficenec, J. A., Einea, A., & Holdsworth, S. (1993). A new technique to create continuity in prestressed concrete members. *PCI Journal*, 38(5), 30–37.
- TNO DIANA BV. (2014). *DIANA finite element analysis user's manual release 9.6*. Delft: TNO DIANA BV.
- Vintzileou, E., & Tassios, T. (1986). Mathematical models for dowel action under monotonic conditions. *Magazine of Concrete Research*, 38(134), 13–22.
- Walraven, J. C. (1981). Fundamental analysis of aggregate interlock. *ASCE Journal of the Structural Division*, 107(11), 2245–2270.
- Walraven, J. C., & Reinhardt, H. W. (1981). Theory and experiments on the mechanical behaviour of cracks in plain and reinforced concrete subjected to shear loading. *Concrete Mechanics Part A Heron*, 26(14), 5–68.
- Walraven, J. C., Vos, E., & Reinhardt, H. W. (1979). Experiments on shear transfer in cracks in concrete. Part I: Description of results. *Stevin Laboratory Report* 5-79-3, Delft University of Technology.
- Xu, J., Wu, C., Li, Z. X., & Ng, C. T. (2015). Numerical analysis of shear transfer across an initially uncrack reinforced concrete member. *Engineering Structures*, 102, 296–309.
- Zoubek, B., Fahjan, Y., Fischinger, M., & Isakovic, T. (2014). Nonlinear finite element modelling of centric dowel connections in precast buildings. *Computers and Concrete*, 14(4), 463–477.

## Publisher's Note

Springer Nature remains neutral with regard to jurisdictional claims in published maps and institutional affiliations.

**Submit your manuscript to a SpringerOpen® journal and benefit from:**

- Convenient online submission
- Rigorous peer review
- Open access: articles freely available online
- High visibility within the field
- Retaining the copyright to your article

Submit your next manuscript at ► [springeropen.com](http://springeropen.com)